

## Quantum Monte Carlo study of polyexcitons in semiconductors

A. C. Cancio and Yia-Chung Chang

*Department of Physics, University of Illinois at Urbana-Champaign,  
1110 West Green Street, Urbana, Illinois 61801*

*and Materials Research Laboratory, University of Illinois at Urbana-Champaign, 104 South Goodwin Avenue, Urbana, Illinois 61801*

(Received 19 March 1990; revised manuscript received 19 September 1990)

A variational Monte Carlo method was used to calculate the binding energies and ground-state wave functions of two-, three-, and four-exciton complexes in indirect-band-gap semiconductors within the spherical-effective-mass approximation. The results for two-exciton complexes (biexcitons) have been compared with those of Green's-function Monte Carlo calculations which produce exact ground-state energies within statistical error; the variational results recover about 90% of the binding energy of these systems. For three- and four-exciton complexes in Si, we predict that the binding energy with respect to the smaller complex with one less exciton is about 2.2 meV, in fair agreement with the experimental value of 2.5 meV.

### I. INTRODUCTION

Si and Ge are host at low temperatures to a large variety of excitonic complexes, stably bound systems of electrons and holes which are analogs of hydrogenic and positronium systems, the primary effect of the surrounding crystal being to adjust the effective masses of the particles and the dielectric constant of the Coulomb interaction.<sup>1</sup> The biexciton  $X_2$ , an analog of the positronium molecule consisting of two electron-hole pairs, has been observed in photoluminescence spectra in Si (Refs. 2 and 3) and stressed Ge,<sup>4</sup> and thermodynamic measurements of the biexciton gas have been made in a strain well in Si.<sup>5</sup> Theoretical studies have included variational<sup>6</sup> and Green's-function Monte Carlo<sup>7</sup> calculations. Bound multiexcitonic complexes consisting of several excitons bound to a shallow impurity have also been found in Si (Refs. 1, 8, and 9) and have been studied theoretically with configuration-interaction<sup>10</sup> and density-functional methods.<sup>11</sup> The electron-hole liquid (EHL) (Ref. 12) is the most stable phase in the thermodynamic limit at low temperatures.

The chief characteristic that provides the stability of the larger systems, in contrast to positron-electron systems, is the large degeneracy of the electron and hole band extrema that permits a large number of both electrons and holes to occupy low-energy states without the violation of Fermi statistics. For this reason it would appear that one should also expect to find a series of stable free complexes of several excitons, or polyexcitons analogous to the BMEC's bound to impurity centers.<sup>13</sup> The series would consist of, in addition to the biexciton, the triexciton or  $X_3$  consisting of three electron-hole pairs and the quadriexciton ( $X_4$ ) with four electrons and holes, as well as larger complexes, up to the filling of the electron degeneracy at  $N=12$  for Si and  $N=8$  for Ge. However, no clear experimental evidence of the existence of polyexcitons has existed until recently, due to unfavorable kinetics of formation in the presence of the EHL at low temperatures, and the difficulty of resolving the ki-

netic energy broadened line shapes of these complexes in phonon-assisted photoluminescence spectra. Recently Steele *et al.*<sup>14</sup> have circumvented these obstacles by studying the luminescence spectra associated with two-electron-hole pair recombination in Si at temperatures higher than the EHL critical point at 20 K and have obtained good estimates of the binding energy of the  $X_2$ ,  $X_3$ , and  $X_4$ .

Over the past 20 years there has been much growth in the use of Monte Carlo methods to study the ground-state properties of quantum systems.<sup>15</sup> In particular, variational Monte Carlo (VMC) uses the Metropolis random-walk algorithm<sup>18</sup> to calculate the expectation values of trial wave functions in a standard variational calculation, greatly enhancing the ability of variational methods to handle many-body systems.<sup>15-17</sup> A more powerful method, Green's-function Monte Carlo (GFMC),<sup>15,21</sup> uses a random-walk method to project out the lowest eigenvalue component of an initial trial wave function, and in principle can determine the ground-state energy of a boson Hamiltonian exactly. Recent calculations of atoms, molecules, and the electron gas have employed both the VMC (Refs. 19 and 20) method and GFMC (Refs. 21-23) and the biexciton has been studied with diffusion Monte Carlo,<sup>7</sup> a variant of GFMC.

In this paper we report the first theoretical calculation of the ground-state properties of the  $X_3$  and  $X_4$  polyexcitons in the spherical-effective-mass approximation, using variational Monte Carlo. In Secs. II and III we discuss the theoretical background of our calculation, the Hamiltonian, and variational wave function, respectively. Section IV is a review of the VMC method and discusses how to obtain expectation values for the ground state. Sections V and VI present our numerical results for binding energy and density of the complexes, and Sec. VII is a summary of our conclusions.

### II. HAMILTONIAN

A simple qualitative picture of a multiexciton system is that of electrons and holes occupying the states in the vi-

cinity of the conduction- and valence-band extrema, weakly coupled by a Coulomb interaction screened by the crystal dielectric constant:  $V(r_{ij})=Z_i Z_j / \epsilon r_{ij}$ . In indirect semiconductors such as Si and Ge, both the electron and hole bands have degenerate extrema. In particular, the hole band maximum at  $\mathbf{k}=0$  has a fourfold degeneracy, corresponding to a state with spin  $\frac{3}{2}$  and the electron band has six (four) minima at nonzero  $\mathbf{k}$  in the [100] ([111]) and equivalent directions for Si (for Ge). Therefore, up to four holes and up to twelve or eight electrons can occupy band extrema states before the effect of Pauli exclusion lifts particles to states of higher energy. This multiple degeneracy is especially important for the stability of systems of three or more excitons.

There are two major hurdles facing the theoretical calculation of the properties of multiexcitonic systems. One problem is the difficulty of treating all the relevant details of the crystal band structure that occur in the general effective-mass formulation of an electron-hole Hamiltonian,<sup>24</sup> including the coupling of degenerate bands at the valence-band maximum, the valley-orbit interaction, and the anisotropy of the conduction band. Accurate calculations of the low-lying exciton states in a realistic model of an indirect semiconductor have been done,<sup>25</sup> but the extension to larger systems, especially those with several holes, would be a formidable task. At the same time, a fairly reasonable estimate of exciton properties can be made in many semiconductors with a simple effective-mass model. The other difficulty is the proper treatment of the correlation energy of these finite many-body systems, which is essential in obtaining accurate binding energies. The large number of independent variables, none of which are negligible or adiabatic for the values of the effective masses relevant to experiment, makes a quantitatively accurate solution of the Schrödinger equation for systems of two or more excitons extremely difficult. Furthermore, the binding energies of these systems are typically only a small fraction of the total ground-state energy, and are thus difficult to predict quantitatively. So far the most accurate calculation on biexcitons has been the GFMC calculation of Ref. 7. In comparison, the existing variational calculations<sup>6</sup> obtained only about 50% of the correlation energy.

Given a focus on the role of interparticle correlations in these systems, the spherical-effective-mass model serves as a useful starting point. The kinetic energy of electrons in the vicinity of the conduction-band minimum and of holes near the valence-band maximum are parametrized by a spherical effective electron mass  $m_e$  and hole mass  $m_h$ , in  $r$ -space representation,

$$\begin{aligned} H_e(-i\nabla) &= \frac{\hbar^2}{2m_e} \nabla^2, \\ H_h(-i\nabla) &= \frac{\hbar^2}{2m_h} \nabla^2. \end{aligned} \quad (1)$$

TABLE I. Spherical-effective-mass parameters for Si, from Ref. 26. Mass in units of the free-electron mass,  $m_0$  length in angstroms, energies in meV.

Crystal	$m_e/m_0$	$m_h/m_0$	$\sigma$	$\mu_{eh}/m_0$	$\epsilon$	$a_X$ (Å)	$E_X$ (meV)	$a_{\text{expt}}$ (Å)	$E_{\text{expt}}$ (meV)
Si	0.2588	0.234	1.11	0.123	11.4	49.0	12.88	44.3	14.7

The Hamiltonian of a multiexcitonic system in this approximation reduces to the equivalent of an electron-positron or hydrogenic system, with natural units of exciton radius,  $a_X = \hbar^2 / (2\mu_{eh} e^2 / \epsilon)$ , and exciton Rydberg,  $E_X = \mu_{eh} e^4 / 2e^2 \hbar^2$ , where  $\mu_{eh} = m_e m_h / (m_e + m_h)$  is the exciton reduced mass. For a system with  $N$  electrons and  $N$  holes, the Hamiltonian in these units is given by

$$\begin{aligned} H = & \sum_{i=1}^N \left[ -\frac{1}{1+\sigma} \nabla_i^2 \right] + \sum_{j=1}^N \left[ -\frac{\sigma}{1+\sigma} \nabla_j^2 + \right] \\ & + \sum_{i=1}^N \sum_{\substack{i'=1 \\ (i'<i)}}^N \frac{2}{r_{ii'}} + \sum_{j=1}^N \sum_{\substack{j'=1 \\ (j'<j)}}^N \frac{2}{r_{jj'}} - \sum_{i=1}^N \sum_{j=1}^N \frac{2}{r_{ij}}, \end{aligned} \quad (2)$$

with  $\sigma = m_e / m_h$ , the electron- to hole-mass ratio, the only crystal-dependent parameter of the model. The electron coordinates are denoted by  $\mathbf{r}_i$  (or  $\mathbf{r}_{i'}$ ) and the hole coordinates are denoted by  $\mathbf{r}_j$  (or  $\mathbf{r}_{j'}$ ). Reference values to spherical-effective-mass parameters and the experimental exciton Bohr radius and Rydberg are given in Table I. The exciton Rydberg in the spherical approximation, 12.88 meV, is in fairly good agreement with the experimental ground-state energy of 14.7 meV.

### III. VARIATIONAL WAVE FUNCTION

As a finite system, the polyexciton should exhibit the properties of both high-density and low-density phases of the corresponding infinite system, in this case the metallic EHL and the exciton gas. The phase transition between the two is both a liquid-gas transition and a metal-insulator transition, in which the quasiparticles of the low-density phase, the excitons, disassociate into their component parts at high densities to form a two-component liquid. For a polyexciton one expects that interparticle correlations for particles near the center of the polyexciton should resemble those of the liquid, while particles farther away from the center should tend to group into excitons. A standard wave function suitable for a liquid, and ignoring Pauli exclusion, is the Jastrow form, a product of pair-correlation functions. Taking into account different correlation functions  $f_{ee}$ ,  $f_{eh}$ ,  $f_{hh}$ , for electron-electron, electron-hole, and hole-hole interactions, respectively, the Jastrow wave function of a system with  $N_e$  electrons and  $N_h$  holes is

$$\psi_J(R) = \prod_{i=1}^{N_e} \prod_{i'=1}^{N_e} f_{ee}(r_{ii'}) \prod_{j=1}^{N_h} \prod_{j'=1}^{N_h} f_{hh}(r_{jj'}) \prod_{i=1}^{N_e} \prod_{j=1}^{N_h} f_{eh}(r_{ij}), \quad (3)$$

where  $R = (\mathbf{r}_1^e, \dots, \mathbf{r}_{N_e}^e; \mathbf{r}_1^h, \dots, \mathbf{r}_{N_h}^h)$ , and  $r_{ij}$  is the distance between the  $i$ th and  $j$ th particles. This form incorporates simply and elegantly the two-particle correlations induced in the wave function by the potential ener-

gy, in particular the cusps in the wave function due to the singularity in the Coulomb potential that occur as two particles approach each other. It lacks, however, the flexibility to allow for the unscreened excitonic correlation one expects for electron-hole pairs at the surface of the polyexciton in addition to the screened electron-hole correlation appropriate for high-density regions.

At low density the wave function for the  $X_N$  approaches that of  $N$  free excitons,

$$\psi_{NX}(R) = \sum_P \prod_{i=1}^N \phi_X^0(|\mathbf{r}_i^e - \mathbf{r}_{P(i)}^h|), \quad (4)$$

where the sum is over all permutations of the hole indices and  $\phi_X^0$  is the exciton ground-state wave function. A wave function suitable for both regimes is the product of the Jastrow and free-exciton forms, which can be written as

$$\psi_{X_j}(R) = \psi_j(R) \sum_P \prod_{i=1}^N \eta(|\mathbf{r}_i^e - \mathbf{r}_{P(i)}^h|), \quad (5)$$

$$\eta(r) = f_X(r) / f_{eh}(r). \quad (6)$$

This form improves the variational estimate of the energy considerably, especially for the  $X_2$ , but rapidly grows cumbersome, since the number of permutations grows as  $N!$ . On the other hand, the relative importance of low-density asymptotic configurations also decreases with the size of the system.

The trial wave function is symmetric under the exchange of electrons or of holes, as is required for the ground state of systems with no more than four holes and twelve electrons. For larger complexes the antisymmetrization required by Fermi statistics can be incorporated by multiplying expression (3) by a product of Slater determinants of single-particle wave functions (including spin), one for each separate electron or hole degeneracy state.

The asymptotic behavior of the ground state can be accounted for in part either by the pair-correlation functions or by including a product of single-particle wave functions  $\phi(|\mathbf{r}_i - \mathbf{r}_{c.m.}|)$  centered about the center of mass  $r_{c.m.}$ .

We must now determine variational forms for two electron-hole correlation functions,  $f_X$  and  $f_{eh}$ , as well as hole-hole and electron-electron functions. The behavior of the correlation functions at short distances can be largely optimized using cusp conditions. As the distance  $r$  between any two particles interacting through a Coulomb potential goes to zero, the eigenstates must have a cusp in  $r$  producing a singularity in the kinetic energy that cancels out the  $1/r$  singularity in the potential. The Jastrow form can satisfy this cusp condition exactly by imposing the following condition on the short-range behavior of the appropriate particle-particle correlation function  $f_{\alpha\beta}(r)$ :

$$\lim_{r \rightarrow 0} \left[ \frac{d}{dr} \ln f_{\alpha\beta}(r) \right] = Z_\alpha Z_\beta \mu_{\alpha\beta}, \quad (7)$$

where  $\mu_{\alpha\beta}^{-1} = m_\alpha^{-1} + m_\beta^{-1}$  is the reduced mass of the interaction, and  $Z_\alpha$  and  $Z_\beta$  are the charges of the two particles. Inclusion of this property into the trial wave func-

tion greatly reduces the variance of the local energy discussed in Sec. IV, with corresponding improvement in the efficiency of statistical methods of calculating its expectation value.

For interparticle distances much larger than the exciton radius, one expects that the Jastrow correlation functions show the effects of screening by other particles, while  $f_X$  stays fairly close to the exciton ground state. We use an effective generalized Schrödinger equation for each kind of particle-particle interaction and solve for  $f_{\alpha\beta}(r)$  numerically:

$$[H_{\alpha\beta} - \lambda_{\alpha\beta}(r)]f_{\alpha\beta}(r) = 0, \quad (8)$$

$$H_{\alpha\beta} = -\frac{1}{\mu_{\alpha\beta}} \nabla^2 + \frac{2Z_\alpha Z_\beta}{r}. \quad (9)$$

The energy function that satisfies this equation is given by

$$\begin{aligned} \lambda_{\alpha\beta}(r) = & \Lambda_{\alpha\beta} \exp(-r^2/r_{sc}^2) \\ & + \exp(k_{\alpha\beta}r) H_{\alpha\beta} \exp(-k_{\alpha\beta}r) [1 - \exp(-r^2/r_{sc}^2)], \end{aligned} \quad (10)$$

$\Lambda_{\alpha\beta}$  is determined by requiring that  $\lim_{r \rightarrow 0} [r f_{\alpha\beta}(r)] = 0$  and the screening length  $r_{sc}$  and the  $k_{\alpha\beta}$  for the different types of interactions are variational parameters.

The correlation function thus generated satisfies the Coulomb cusp condition at  $r=0$  and approaches the asymptotic form  $\exp(-k_{\alpha\beta}r)$  for distances much larger than  $r_{sc}$ . Other long-range forms were also tried, but the ground-state energy proves to be largely insensitive to the exact form used.

#### IV. VARIATIONAL MONTE CARLO

The variational approach to finding the ground state of an  $N$ -particle system involves evaluating the energy expectation value of a trial ground-state wave function,

$$\langle E \rangle = \frac{\int dR |\psi(R)|^2 E(R)}{\int dR |\psi(R)|^2}, \quad (11)$$

$$E(R) = \psi^{-1}(R) [H \psi(R)], \quad (12)$$

where  $R$  is the coordinate of the  $3N$ -dimensional configuration space,  $\{\mathbf{r}_1, \mathbf{r}_2, \dots, \mathbf{r}_N\}$ , and  $dR$  denotes integration over the configuration space volume element,  $d^3r_1 d^3r_2 \dots d^3r_N$ . In a variational Monte Carlo approach one uses a random-walk algorithm to sample a population of random points  $R_i$  in configuration space from the probability distribution  $|\psi(R)|^2 / \int dR |\psi(R)|^2$ .

Given a set of  $M$  configurations,  $\{R_i\}$ , the expectation value  $\langle O \rangle$  of any operator  $O(R)$  defined as in Eqs. (11) and (12) can be estimated as

$$\langle O \rangle = \frac{1}{M} \sum_{i=1}^M O(R_i) + O(1/\sqrt{M}). \quad (13)$$

The error of such an estimate, assuming that the random configurations are statistically independent, is roughly

$\sigma_0/\sqrt{M}$ , where  $\sigma_0^2$  is the variance  $\langle O^2 \rangle - \langle O \rangle^2$  of the local operator  $O(R)$ . Thus the convergence rate of the calculation depends only on the size of the variance and the computer time necessary to calculate  $O(R)$  and  $\psi(R)$  for each configuration.

The calculation of the energy expectation value is particularly stable since the variance of the local energy  $E(R)$  vanishes as the trial wave function approaches an eigenfunction of the Hamiltonian and  $E(R)$  tends to the corresponding eigenvalue for all  $R$ . It is thus crucial to choose the trial wave functions close enough to the ground state that not only is the energy expectation value close to the ground-state energy, but also the local energy is slowly varying and roughly the same order of magnitude everywhere in configuration space. This property of the variance can also be used as an alternate variational principle for optimizing the wave function.<sup>20</sup>

The generation of configurations sampled from the probability distribution  $|\psi(R)|^2/\int dR |\psi(R)|^2$  is achieved by the following random-walk algorithm. Given a member  $R_i$  of the set of sample configurations, a trial configuration  $R'_i$  is generated, and one of these configurations is chosen to be the next configuration in the set according to the following rule:

$$R_{i+1} = \begin{cases} R'_i, & \frac{|\psi(R'_i)|^2}{|\psi(R_i)|^2} + \xi > 1 \\ R_i, & \frac{|\psi(R'_i)|^2}{|\psi(R_i)|^2} + \xi < 1, \end{cases} \quad (14a)$$

$$R_{i+1} = \begin{cases} R'_i, & \frac{|\psi(R'_i)|^2}{|\psi(R_i)|^2} + \xi > 1 \\ R_i, & \frac{|\psi(R'_i)|^2}{|\psi(R_i)|^2} + \xi < 1, \end{cases} \quad (14b)$$

where  $\xi$  is a uniform random number between 0 and 1. The trial configuration is typically generated by moving one or more particles to new sites chosen at random within boxes centered about their old positions. The size of box used is adjusted so that the probability of choosing the trial configuration is roughly  $\frac{1}{2}$ . The probability distribution of configurations generated by this random walk converges to the desired probability distribution after allowing an equilibration time of a short number of steps (between 10 to 30 for the present calculation) to avoid any transient effects from the initial configuration.

## V. GROUND-STATE ENERGY

To test the quality of the variational theory and our computer program, variational calculations were first carried out on hydrogenic systems for which essentially exact results are available. For the hydrogen ion  $H^-$  we obtain a best value for the ground-state energy of  $-1.0540(5)$  Ry as compared with the exact value of  $-1.0555$  Ry (Ref. 26); for the hydrogen molecule  $H_2$ , we obtain  $-2.335(2)$  Ry as compared to the variational value of  $-2.347$  Ry (Ref. 27); for the positronium molecule  $(Ps)_2$ , consisting of two electrons and two positrons, and analogous to the biexciton at  $\sigma=1$ , the present theory gives  $-1.025(1)$  Ry as compared to  $-1.030(1)$  Ry calculated by a GFMC method.<sup>7</sup> In each case the variational theory recovers more than 99.5% of the total energy; this

is sufficient to obtain binding energies within 5% of the exact values for the hydrogenic systems, but only within 15% for  $(Ps)_2$ .

The binding energies  $W_N(\sigma)$  of the  $X_2$ ,  $X_3$ , and  $X_4$  with respect to the corresponding  $N$ -free-exciton state are plotted in Fig. 1 as a function of the electron-hole mass ratio  $\sigma$  in units of  $E_X$ . With this convention, the binding energy of the  $X_N$  with respect to the  $X_{N-1}+X$  state is the difference between the  $X_N$  and  $X_{N-1}$  curves. In each case the binding energy varies slightly over most of the range of  $\sigma$  and then drops off sharply in the adiabatic region  $\sigma < 0.1$ . This is in agreement with the behavior of  $W_N(\sigma)$  that can be derived from the application of general dimensional arguments.<sup>28</sup> In particular, the polyexciton Hamiltonian is invariant with respect to exchanging the electron and hole masses, so that the binding energy at  $1/\sigma$  is equal to that for  $\sigma$  with the slope of  $W_N(\sigma)$  equaling 0 at the symmetry point  $\sigma=1$ . One expects similar insensitivity to perturbations away from the spherical-effective-mass Hamiltonian in the description of the real crystal.

In Table II, the polyexciton ground state energies for  $\sigma=1$  are listed, as well as the variational and experimental values for the binding energy. The discrepancy between the calculated and observed energies for  $X_3$  and  $X_4$  is consistently 0.3 meV per exciton; the binding energy of each complex increases by approximately 2.2 meV per additional exciton as compared with 2.5 meV observed experimentally.

Typically 10 000 configurations were needed to calculate energy expectation values to four significant digits. These were grouped into 10 independent runs in order to estimate the statistical error of the calculation. The variational parameters were minimized using the method of correlated estimates<sup>15,17</sup> to reduce the statistical uncertainty of the relative difference in energies evaluated from different sets of values of the variational parameters.

## VI. PARTICLE DISTRIBUTION IN POLYEXCITONS

In order to obtain some understanding of the shape and size of polyexcitons, the average density of electrons and holes as a function of distance from the center of mass has been calculated. These functions are defined as

$$\rho_e(\mathbf{r}) = \left\langle \sum_{i=1}^{N_e} \delta(\mathbf{r}_i^e - \mathbf{r}) \right\rangle, \quad (15)$$

$$\rho_h(\mathbf{r}) = \left\langle \sum_{i=1}^{N_h} \delta(\mathbf{r}_i^h - \mathbf{r}) \right\rangle, \quad (16)$$

where particle coordinates are measured in the center-of-mass frame. The rotational invariance of the Hamiltonian with respect to the center of mass indicates that these will be functions of radial distance only, so that one need consider only the spherical averages  $\rho_e(r)$  and  $\rho_h(r)$ . In particular, we concentrate on the  $\sigma=1$  limit, i.e., equal electron and hole masses. In this case, the electron and hole density functions are identical and the interesting quantity will be the total density  $\rho(r) = \rho_e(r) + \rho_h(r)$ .

TABLE II. Polyexciton ground-state energies for  $\sigma = 1$ , and binding energies. VMC ground-state energy  $E_{g\text{VMC}}$  is listed in units of the exciton Rydberg. Statistical uncertainties in the last digit are given in parentheses. VMC binding energies  $W_{\text{VMC}}$  are in meV, using the conversion factor  $1 \text{ Ry} = 14.7 \text{ meV}$ . Experimental binding energies in meV,  $W_{\text{expt}}$ , are from Ref. 14.

Complex	$E_{g\text{VMC}}/E_X$	$W_{\text{VMC}}$ (meV)	$W_{\text{expt}}$ (meV)
$X_2$	-2.050(2)	0.74	1.36
$X_3$	-3.247(5)	2.90	3.83
$X_4$	-4.589(6)	5.03	6.34

One can use Monte Carlo methods to evaluate expectation values such as  $\rho(r)$  defined as a continuous function of  $r$ , with the *caveat* that an approximate discrete evaluation of the  $\delta$  function in the definition of the density operator is taken. This is achieved by partitioning space into a finite number of discrete bins, and calculating the average density of particles in each bin. In particular, since  $\rho(r)$  is spherically symmetric, a partitioning of space into spherical shells of width  $\Delta r$  is used. Then, given a set of  $M$  configurations generated by the Monte Carlo procedure, the number of particles that fall inside a given bin is tallied and averaged over the total number of

configurations. This procedure produces the variational expectation value  $N(r)$  for the average number of particles lying within a spherical shell of width  $\Delta r$  and radius  $r$ . To obtain the density, one must divide this number by the volume of the shell,

$$\rho(r) = N(r) / 4\pi r^2 \Delta r . \quad (17)$$

In practice,  $\Delta r$  is chosen to be the same for each shell, and its value chosen to balance the statistical error of the calculation of  $\rho$  in the region in which most of the particles are concentrated, and the loss of information caused by binning. Finally, as a measure of the size of a complex, the average distance of each particle from the center of mass can also be calculated, either as

$$\langle r \rangle = \left\langle \frac{1}{N} \sum_{i=1}^N r_i \right\rangle \quad (18)$$

or by using the VMC measurement of  $\rho(r)$  and the relation

$$\langle r \rangle = \frac{1}{N} 4\pi \int r^2 r \rho(r) dr . \quad (19)$$

Figure 2 shows the VMC calculation of the density of the  $X_2$ ,  $X_3$ , and  $X_4$  systems as a function of distance from the center of mass. The error bars represent the statisti-

## Polyexciton Binding Energy

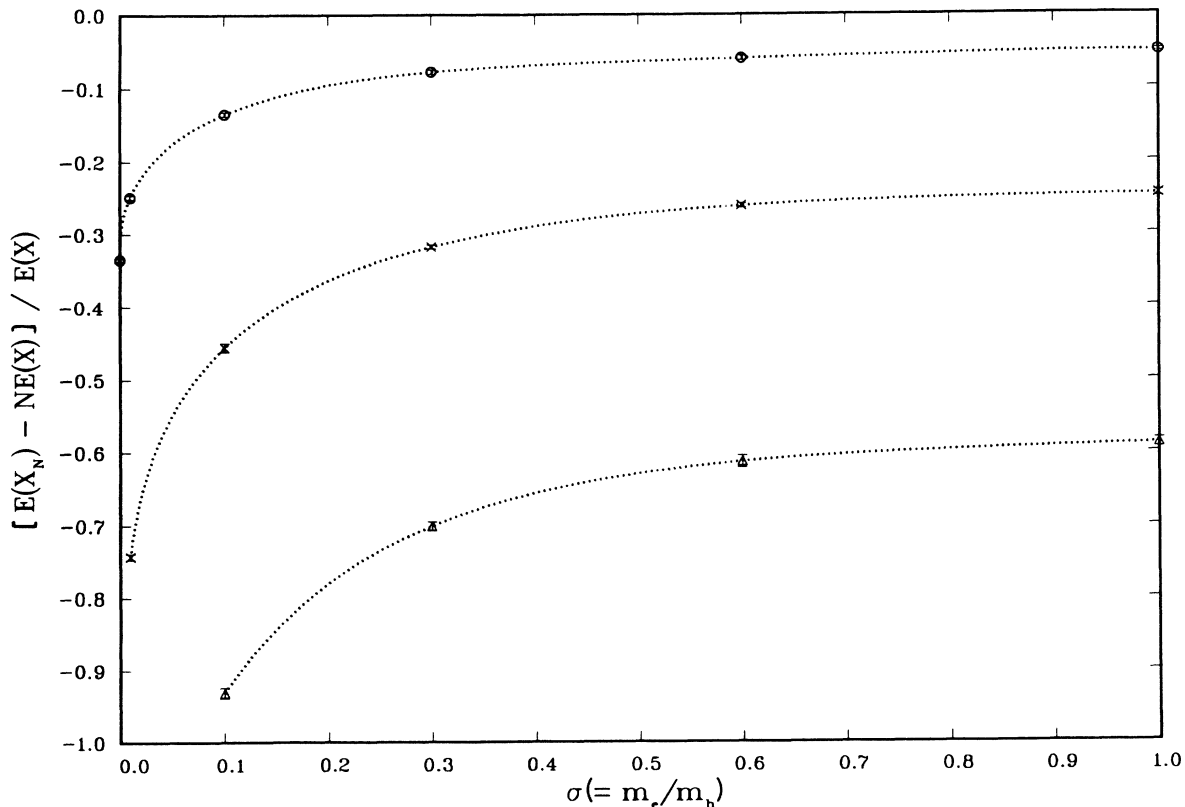


FIG. 1. Binding energy with respect to dissociation into free excitons of the  $X_2$ ,  $X_3$ , and  $X_4$  complexes in units of the exciton Rydberg  $E_X$ . Circles refer to the  $X_2$ , crosses to the  $X_3$ , and triangles to the  $X_4$ .

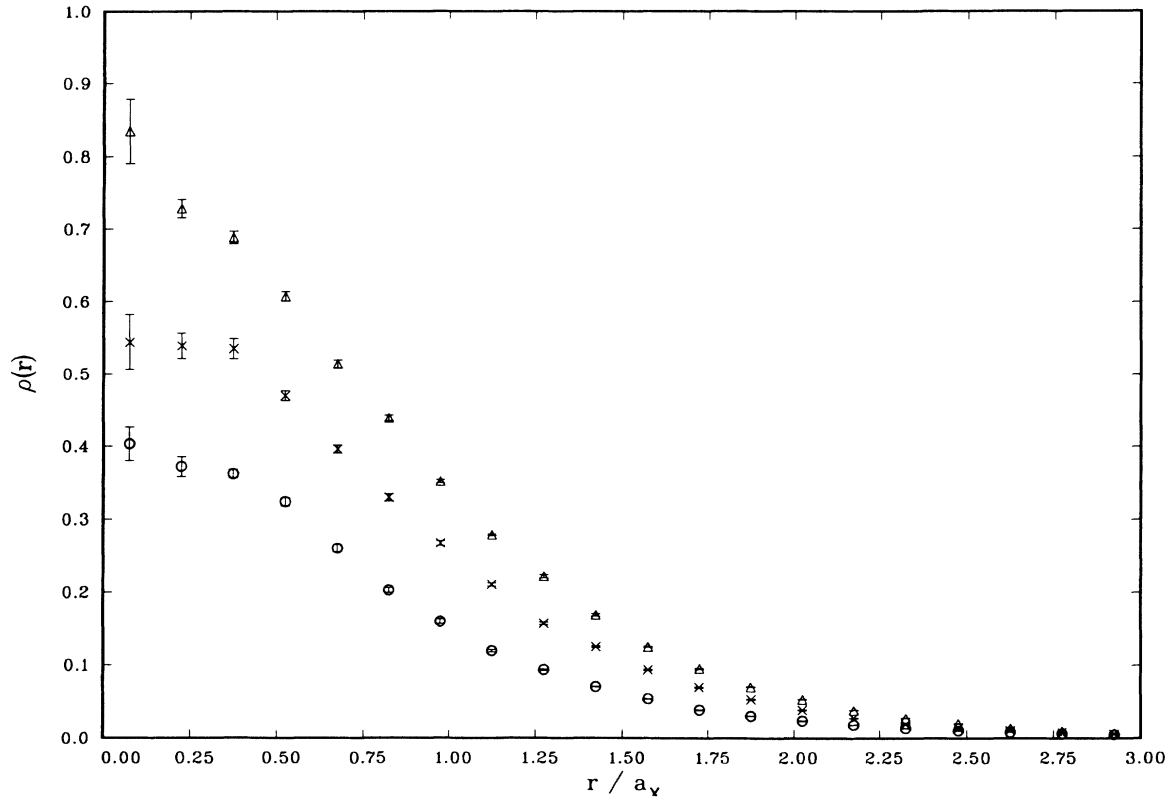
$X_N$  Density

FIG. 2. Particle density as a function of distance from the center of mass for the  $X_2$ ,  $X_3$ , and  $X_4$  complexes. Circles refer to the  $X_2$ , crosses to the  $X_3$ , and triangles to the  $X_4$ .

cal error estimated from ten independent runs. The error is largest at  $r=0$  because of the relatively few particle coordinates that fall within the smaller volume bins as  $r$  tends to zero. It is interesting to compare the polyexciton density profiles with that of the exciton which can be calculated exactly from the ground state, given by

$$\rho(r) = 2 \langle 0 | \delta(\mathbf{r} - (\mathbf{r}^e - \mathbf{r}^h)/2) | 0 \rangle \quad (20)$$

which is proportional to  $e^{-4r/a_X}$ . At small  $r$ , the polyexciton density varies approximately like a Gaussian distribution, in contrast to that of the exciton, which has a cusp at  $r=0$  due to the Coulomb singularity that dominates the behavior of the two-particle system at  $r=0$ . The density at the center of each system  $\rho(0)$  is roughly 0.4, 0.6, and 0.8 for the two-, three-, and four-exciton systems, respectively. At long range it dies off exponentially with a decay width for each case roughly twice as large as that of the exciton.

A clearer comparison of the shape and size of each complex in the region of peak probability can be obtained with the radial probability function, given by  $P(r) = 4\pi r^2 \rho(r) / N$  for a system with  $N$  excitons. Plotted

in Fig. 3, the radial probability densities for the  $X_2$ ,  $X_3$ , and  $X_4$  are nearly identical, with a peak at roughly  $1.15a_X$  as compared with  $0.5a_X$  for the exciton. A more statistically accurate estimate for the radius of the polyexcitons is the mean particle distance from the center of mass, listed in Table III. The radius of each polyexciton is roughly independent of the number of excitons in the complex, and is twice that of the exciton. In comparison, Steele *et al.*<sup>14</sup> have obtained rough estimates of 100, 100, and 130 Å for the  $X_2$ ,  $X_3$ , and  $X_4$  radii by fitting the experimental line shapes to a simple theoretical model.<sup>29</sup>

These estimates for the radii of the polyexcitons indicate a polyexciton volume about eight times that of the

TABLE III. VMC expectation value of particle distance from center of mass, in units of exciton radius. Uncertainties in the last digit are given in parentheses.

Complex	$\langle r \rangle / a_X$
$X_1$	0.750
$X_2$	1.76(3)
$X_3$	1.59(2)
$X_4$	1.57(1)

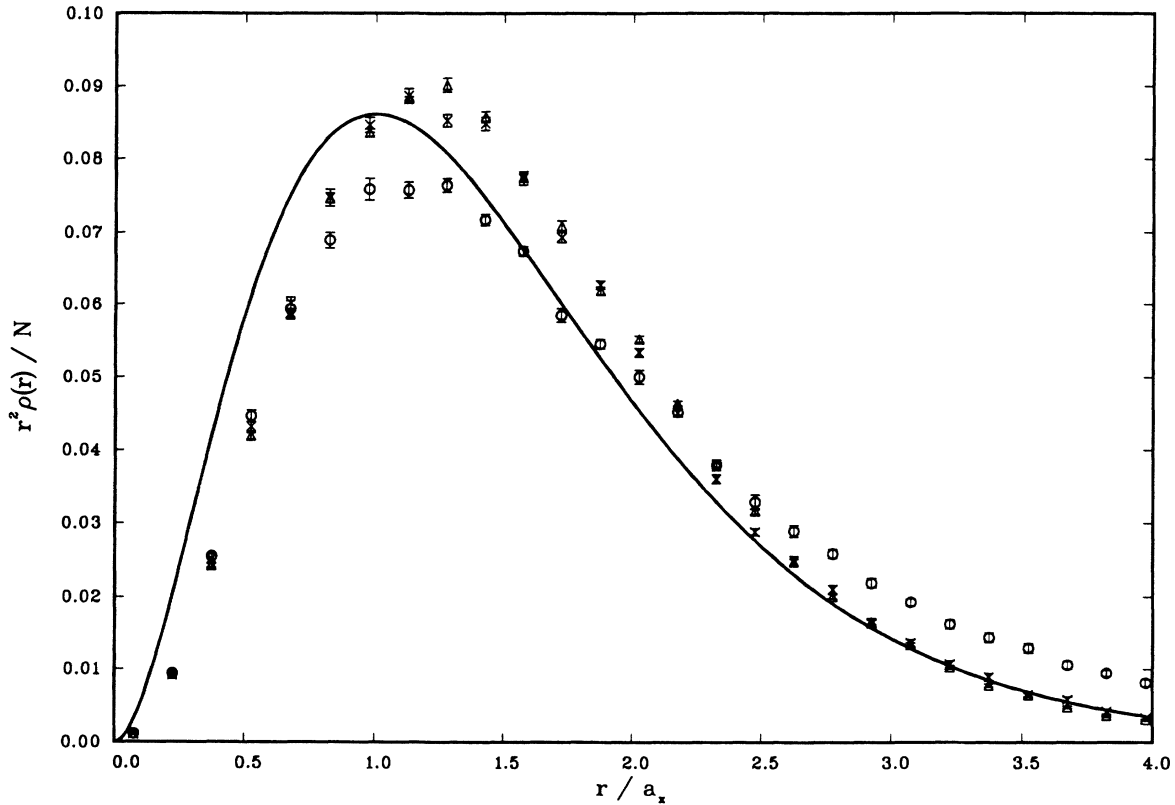


FIG. 3. Radial probability density for the  $X_2$ ,  $X_3$ , and  $X_4$  systems. Circles refer to the  $X_2$ , crosses to the  $X_3$ , and triangles to the  $X_4$ ; solid line is fit to an exciton density with Bohr radius  $2a_x$ .

exciton, with a consequent reduction of the average density of particles. This indicates that these systems, especially the biexciton, are dominated by configurations resembling a loose collection of excitons, versus a tightly bound complex in which the excitons have completely lost their identity.

## VII. CONCLUSION

We have presented the first theoretical calculation of the ground state of the  $X_3$  and  $X_4$  polyexcitons, using the variational Monte Carlo method and a trial wave function consisting of the exciton-gas wave function modified by a product of pair correlation functions. We find a trend of increasing binding energy per exciton as additional excitons are added to the complex as would be expected for a spherically symmetric and attractive exciton-exciton interaction. The calculated binding energies agree fairly well with those observed experimentally.

We have also calculated the radial probability density of these systems and find that they have almost identical sizes and shapes with radii twice that of the exciton, and a density increasing linearly with the number of excitons.

The low average densities and binding energy per exciton at  $\sigma=1$  suggest the picture of these systems as loosely bound excitons.

Preliminary calculations with a GFMC algorithm have been carried out for the  $X_3$  and  $X_4$ , with an increase in binding energy of about 0.03 and 0.05  $E_x$ , respectively. It would also be interesting to extend this calculation to complexes of up to 12 excitons to investigate the effect of Fermi statistics on their stability.

## ACKNOWLEDGMENTS

We would like to thank V. J. Pandaripandhe and D. Lewart for many fruitful discussions and help with developing algorithms. This work was supported by the U.S. Office of Naval Research (ONR) under Contract No. N00014-89-5-1157. We acknowledge the use of the Cray Research, Inc. X-MP/48 computer at the National Center for Supercomputing Applications at the University of Illinois at Urbana-Champaign, and the computing facilities of the University of Illinois Materials Research Laboratory.

- <sup>1</sup>*Excitons*, edited by M. D. Sturge and E. I. Rashba (North-Holland, Amsterdam, 1982).
- <sup>2</sup>M. L. W. Thewalt and J.A. Rostworoski, *Solid State Commun.* **25**, 991 (1978).
- <sup>3</sup>V. D. Kulakovskii, V. B. Timofeev, and V. M. Edelstein, *Zh. Eksp. Teor. Fiz.* **74**, 372 (1978) [*Sov. Phys.—JETP* **47**, 193 (1978)].
- <sup>4</sup>I. V. Kuckushkin, V. D. Kulakovskii, and V. B. Timofeev, *Pis'ma Zh. Eksp. Teor. Fiz.* **32**, 304 (1980) [*JETP Lett.* **32**, 281 (1980)].
- <sup>5</sup>P. L. Gourley and J. P. Wolfe, *Phys. Rev. B* **20**, 3319 (1979).
- <sup>6</sup>W. F. Brinkman, T. M. Rice, and B. Bell, *Phys. Rev. B* **8**, 1570 (1973); O. Akimoto and E. Hanamura, *J. Phys. Soc. Jpn.* **33**, 1537 (1973).
- <sup>7</sup>M. A. Lee, P. Vashishta, and R. K. Kalia, *Phys. Rev. Lett.* **51**, 2422 (1983).
- <sup>8</sup>G. Kirczenov, *Can. J. Phys.* **5**, 1787 (1987).
- <sup>9</sup>M. L. W. Thewalt, *Can. J. Phys.* **55**, 513 (1977).
- <sup>10</sup>Y.-C. Chang and T. C. McGill, *Phys. Rev. B* **25**, 3963 (1982).
- <sup>11</sup>R. S. Pfeiffer and H. B. Shore, *Phys. Rev. B* **25**, 3897 (1982).
- <sup>12</sup>*Electron Hole Droplets in Semiconductors*, edited by C. D. Jeffries and R. V. Keldysh (North-Holland, Amsterdam 1983); T. M. Rice, in *Solid State Physics*, edited by H. Ehrenreich, F. Seitz, and D. Turnbull (Academic, New York, 1977), Vol. 32.
- <sup>13</sup>J. S. Wang and C. Kittel, *Phys. Lett.* **42A**, 189 (1972).
- <sup>14</sup>A. G. Steele, W. G. McMullan, and M. L. W. Thewalt, *Phys. Rev. Lett.* **59**, 2899 (1987).
- <sup>15</sup>D. M. Ceperley and M. H. Kalos, in *Monte Carlo Methods in Statistical Physics*, edited by K. Binder (Springer-Verlag, Berlin, 1979).
- <sup>16</sup>W. L. McMillan, *Phys. Rev.* **138**, A442 (1965).
- <sup>17</sup>D. Ceperley, G. V. Chester, and M. A. Kalos, *Phys. Rev. B* **16**, 3081 (1977).
- <sup>18</sup>N. Metropolis, A. Rosenbluth, M. Rosenbluth, A. H. Teller, and E. Teller, *J. Chem. Phys.* **21**, 1087 (1953).
- <sup>19</sup>D. Ceperley, *Phys. Rev. B* **18**, 3126 (1978).
- <sup>20</sup>C. J. Umrigar, K. G. Wilson, and J. W. Wilkins, *Phys. Rev. Lett.* **60**, 1719 (1988).
- <sup>21</sup>D. Ceperley and B. J. Alder, *J. Chem. Phys.* **81**, 5833 (1984).
- <sup>22</sup>B. L. Hammond, P. J. Reynolds, and W. A. Lester, *Phys. Rev. Lett.* **61**, 2312 (1988).
- <sup>23</sup>D. M. Ceperley and B. J. Alder, *Phys. Rev. Lett.* **45**, 566 (1980).
- <sup>24</sup>G. Dresselhaus, *Phys. Chem. Solids* **1**, 14 (1956).
- <sup>25</sup>T. P. McLean and R. Loudon, *Phys. Chem. Solids* **13**, 1 (1960); A. Baldereschi and N. O. Lipari, *Phys. Rev. B* **3**, 2497 (1971).
- <sup>26</sup>C. L. Pekeris, *Phys. Rev.* **112**, 1644 (1958).
- <sup>27</sup>H. James and A. S. Coolidge, *J. Chem. Phys.* **1**, 825 (1933).
- <sup>28</sup>R. K. Wehner, *Solid State Commun.* **7**, 457 (1969).
- <sup>29</sup>K. Cho, *Opt. Commun.* **8**, 412 (1973).